

## Accepted Manuscript

Sonochemical oxidation of vanillyl alcohol to vanillin in the presence of a cobalt oxide catalyst under mild conditions

Ronan Behling, Grégory Chatel, Sabine Valange

PII: S1350-4177(16)30383-2

DOI: <http://dx.doi.org/10.1016/j.ultsonch.2016.11.015>

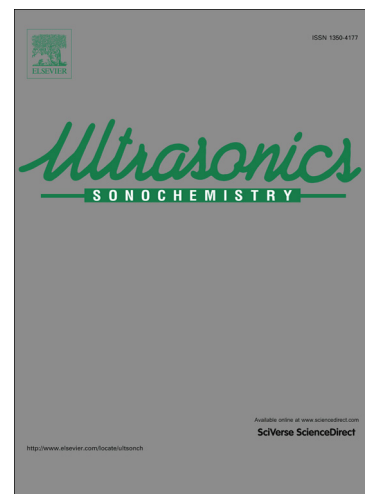
Reference: ULTSON 3429

To appear in: *Ultrasonics Sonochemistry*

Received Date: 23 August 2016

Revised Date: 2 November 2016

Accepted Date: 8 November 2016



Please cite this article as: R. Behling, G. Chatel, S. Valange, Sonochemical oxidation of vanillyl alcohol to vanillin in the presence of a cobalt oxide catalyst under mild conditions, *Ultrasonics Sonochemistry* (2016), doi: <http://dx.doi.org/10.1016/j.ultsonch.2016.11.015>

This is a PDF file of an unedited manuscript that has been accepted for publication. As a service to our customers we are providing this early version of the manuscript. The manuscript will undergo copyediting, typesetting, and review of the resulting proof before it is published in its final form. Please note that during the production process errors may be discovered which could affect the content, and all legal disclaimers that apply to the journal pertain.

**Sonochemical oxidation of vanillyl alcohol to vanillin in the presence of a cobalt oxide catalyst under mild conditions**

Ronan Behling <sup>a</sup>, Grégory Chatel <sup>a,b,\*</sup>, Sabine Valange <sup>a,\*</sup>

<sup>a</sup> *Institut de Chimie des Milieux et Matériaux de Poitiers (IC2MP), Université de Poitiers, CNRS, ENSIP, B1, 1 rue Marcel Doré, F-86073 Poitiers Cedex 9, France.*

<sup>b</sup> *Current address: Laboratoire de Chimie Moléculaire et Environnement (LCME), Université Savoie Mont Blanc, 73376 Le Bourget du Lac Cedex (France)*

\* Corresponding authors:

E-mail addresses: gregory.chatel@univ-smb.fr (G. Chatel), sabine.valange@univ-poitiers.fr (S. Valange)

**Abstract**

The heterogeneous selective oxidation of vanillyl alcohol into vanillin was investigated on new grounds under eco-friendly conditions in the presence of hydrogen peroxide as an oxidant and water as solvent, coupled with low frequency ultrasonic irradiation. The sono-Fenton-like-assisted vanillyl alcohol oxidation was performed with a high-surface area nanostructured spinel cobalt oxide catalyst exhibiting small crystallites size. The catalytic reaction was also carried out under conventional heating conditions for comparison purposes. The influence of the reaction parameters, namely catalyst loading and hydrogen peroxide concentration was studied with the aim of determining the optimum yield and selectivity to the desired vanillin product. The chemical effects of ultrasound (ability to generate hydroxyl radicals) along with increased mass transfer appeared to be key prerequisites for enhancing the efficiency of the process, while decreasing the overall energy consumption.

**Keywords:** Selective oxidation; Sonochemistry; Ultrasound; Hydrogen peroxide; Cobalt oxide catalyst.

## 1. Introduction

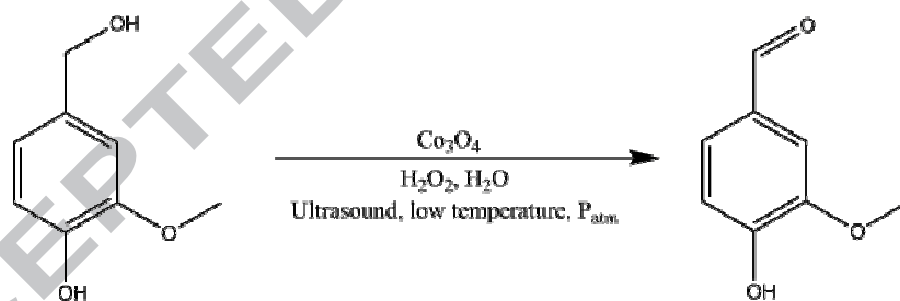
Liquid phase aerobic oxidation of lignin derived sub structure compounds such as monomeric platform alcohols is being explored extensively to prepare functionalized aromatics for the production of a variety of fine chemicals. Among them, the most studied substrates are veratryl, vanillyl, *p*-sinapyl, *p*-coumaryl, coniferyl alcohols and 2-phenoxy-1-phenylethanol [1]. The selective catalyzed oxidation of such aromatic alcohols to the corresponding carbonyl compounds is indeed worthy of interest for plentiful industrial applications. Vanillyl alcohol (VA) can be selectively oxidized to vanillin, which has a wide range of applications in food and perfumes or as a platform chemical for pharmaceuticals production [2]. Vanillyl-alcohol oxidase and laccase-catalyzed reactions have been reported for the selective production of vanillin [3,4]. Direct routes to vanillin are also well explored through conventional soxhlet extraction, microwave or ultrasound-assisted extraction from vanilla pods [5,6,7].

Conventionally, oxidation of vanillyl alcohol is performed using homogeneous catalysts, including metalloporphyrin, cobalt(salen) and methyltrioxo rhenium complexes, as well as simple metal salt-based catalysts [8]. Heterogeneous catalysts are however preferred over their homogeneous analogs from an environmentally point of view, thereby promoting the atom-efficient synthesis of fine chemicals. The heterogeneous selective oxidation of vanillyl alcohol using molecular O<sub>2</sub> as a primary oxidant has been widely studied. The group of Rode has deeply investigated the use of cobalt-based catalysts, such as Co<sub>3</sub>O<sub>4</sub> and Mn-Co mixed oxides (supported or not) for the selective oxidation of VA and similar platform monoaromatic substrates under pressures until 4 MPa and temperatures around 150-160 °C [9]. Alkali-mediated aerobic oxidation of VA into vanillin has also been investigated with cobalt-based zeolitic imidazolate framework catalysts, as well as with Pt and Pd immobilized on various carriers (carbon, MOFs, TiO<sub>2</sub>, SiO<sub>2</sub> and MgO) [1].

The heterogeneously-catalyzed photo-oxidation of aromatic alcohols to aldehydes under sunlight and UV-Vis light was recently comprehensively reviewed [10,11]. Such strategy may lead to relatively short reaction times, at mild conditions without addition of any extra chemicals. The photo-production of vanillin was reported in aqueous medium in the presence of a variety of TiO<sub>2</sub> powders using air or oxygen as a primary oxidant [12].

Studies dealing with the aqueous phase selective oxidation of VA using a heterogeneous catalyst together with  $\text{H}_2\text{O}_2$  as oxidant have however been scarcely reported [1]. Crestini *et al.* immobilized a methyltrioxorhenium complex on low-cost polymeric supports for the hydrogen peroxide selective oxidation of the side chain hydroxyl group of VA with acetic acid as reaction solvent [13]. Such MTO-based catalysts are however toxic for both the environment and human health [14]. Very recently, the liquid phase oxidation of VA into vanillin with  $\text{H}_2\text{O}_2$  was investigated with the use of a cobalt titanate catalyst in various organic solvents at  $85\text{ }^\circ\text{C}$  [15]. The hydrogen peroxide microwave-assisted oxidation of VA was explored in another study with a lanthanum-containing SBA-15 mesoporous silica in acetonitrile [16].

To the best of our knowledge, no data on the combined use of water as solvent and hydrogen peroxide as O-donor for such heterogeneously catalyzed reaction was reported so far. The present study falls within this context with the aim of investigating the hydrogen peroxide oxidation of vanillyl alcohol into vanillin with a non-noble metal based solid catalyst under more eco-friendly conditions (ambient pressure, low temperature and aqueous medium) coupled with low frequency ultrasonic irradiation (US), as unconventional activation route (Scheme 1).



**Scheme 1:** Selective oxidation of vanillyl alcohol into vanillin under ultrasonic and mild conditions in the presence of Co-based heterogeneous catalyst.

In order to evaluate the effects of US on the reaction and the associated oxidation mechanisms, comparative studies were carried out under conventional heating (CH). For that purpose, a nanostructured spinel cobalt oxide ( $\text{Co}_3\text{O}_4$ ) was synthesized *via* a controlled co-precipitation route and fully characterized before and after reaction by several complementary techniques, such as XRD, nitrogen adsorption, TG-DTA, elemental analysis, TPR, scanning and transmission electron microscopy and XPS.

Moreover, sonochemistry could offer new strategies in heterogeneous catalyzed-oxidation reactions through intense mechanical, thermal and chemical effects generally responsible of an increase of reaction rates, changes in reaction mechanisms, emulsification effects, crystallization, precipitation, erosion, etc [17,18]. The formation, growth and the sudden collapse of gaseous microbubbles in the liquid phase, due to the cavitation phenomenon, create locally high temperatures and pressures that can initiate high-energy radical mechanisms and generate physical effects [19,20,21]. Even if the full mechanism has not been elucidated yet, it is usually accepted that low frequencies (20–80 kHz) preferentially lead to physical effects, while high frequencies (150–2,000 kHz) favor the production of radicals. However, it is known that the production of HO• radicals can be improved in water at low frequency in the presence of catalysts through sono-Fenton-like processes [22]. In the present work, the ability of ultrasound to generate *in situ* hydrogen peroxide and hence hydroxyl radicals (chemical effects) and the increase of mass transfer between the Co<sub>3</sub>O<sub>4</sub> catalyst and the substrate (physical effects) will be discussed.

## 2. Experimental

### 2.1. Synthesis of the catalyst

The nanostructured spinel Co<sub>3</sub>O<sub>4</sub> catalyst was prepared by a controlled homogeneous co-precipitation route adapted from the synthesis procedure described by Mate *et al* [23]. Cobalt nitrate hexahydrate was used as Co precursor along with potassium carbonate as precipitating agent. The precipitation step was carried out at a fixed pH of 8.5. Briefly, a 0.03 mol L<sup>-1</sup> solution of Co(NO<sub>3</sub>)<sub>2</sub>·6H<sub>2</sub>O and a 0.06 mol L<sup>-1</sup> solution of K<sub>2</sub>CO<sub>3</sub> were first prepared. The controlled simultaneous addition of 400 mL of each solution to a round bottom flask containing 100 mL of distilled water at 70 °C under constant stirring resulted in the formation of a purple precipitate. The obtained slurry was further aged at 70 °C during 16 h. The resulting solid was recovered by filtration, thoroughly washed with distilled water until all potassium ions have been removed and dried at 100 °C before being calcined at 300 °C for 5 h in a Nabertherm controller P320 muffle oven (heating rate: 2 °C min<sup>-1</sup>).

## 2.2. Selective oxidation reaction

### 2.2.1. Oxidation of vanillyl alcohol under silent conditions

0.2 g (1.3 mmol) of vanillyl alcohol were dissolved in distilled water at 75 °C. After dissolution, the catalyst (4 mg, 2 wt%) was added, followed by the addition under magnetic stirring (1000 rpm) of 1–4 molar equivalents of 30 wt% aqueous hydrogen peroxide solution (135–540  $\mu\text{L}$ ), so that the total volume was 4 mL.

### 2.2.2. Ultrasound-assisted oxidation of vanillyl alcohol

0.2 g (1.3 mmol) of vanillyl alcohol were dissolved in distilled water at 75 °C. After its dissolution, the catalyst (4 mg, 2 wt%) was added, followed by the addition of 1–4 molar equivalents of 30 wt% aqueous hydrogen peroxide solution (135–540  $\mu\text{L}$ ) so that the total volume was 4 mL under ultrasonic irradiation. Ultrasound was generated by a Digital Sonifier<sup>®</sup> S-250D from Branson (power of standby  $P_0 = 27.0$  W, nominal electric power of the generator  $P_{\text{elec}} = 8.2$  W). A 3.2 mm diameter tapered microtip probe operating at a frequency of 19.95 kHz was used. The volume acoustic power of this system was  $P_{\text{acous.vol}} = 0.25$  W.mL<sup>-1</sup> in water (determined by calorimetry measurements) [24] and an average radical formation rate of  $v(\text{I}_3^-) = 1.94 \times 10^{-6}$  mol s<sup>-1</sup> in 4 mL of water (determined by dosimetry method from 0.1 mol L<sup>-1</sup> solution) [25]. The reaction medium (vanillyl alcohol, catalyst, H<sub>2</sub>O<sub>2</sub> and water) was inserted in a rounded cylindrical glass reactor (17 mm in interior diameter, 102 mm in height) and the temperature was not controlled. The ultrasonic probe was directly immersed in the reaction medium. Energy consumption was measured with a wattmeter (Perel<sup>®</sup>).

### 2.2.3. Determination of vanillyl alcohol conversion and vanillin yield

At the end of the reaction, the aqueous solution was diluted, filtered (Fisherbrand<sup>®</sup> PTFE membrane filter with a pore size of 0.45  $\mu\text{m}$ ) and analyzed by a Shimadzu<sup>®</sup> HPLC LC-20AD (injection volume: 10  $\mu\text{L}$ ) equipped with a C18 column (Interchrom UP50DB-250/046 C18-ODB 5  $\mu\text{m}$  250x4.6mm HP) using a Waters<sup>®</sup> 2410 refractive index detector, and a 10/90 acetonitrile/water (V/V) mobile phase with a rate of 0.6 mL min<sup>-1</sup>.

The catalytic performance of the nanostructured spinel Co<sub>3</sub>O<sub>4</sub> catalyst was evaluated in terms of conversion of vanillin alcohol (%) and yield/selectivity (%) to vanillin product, according to Eqs. (1–3):

$$\text{Conversion (\%)} = \frac{\text{Initial moles of VA} - \text{Remaining moles of VA}}{\text{Initial moles of VA}} \times 100\% \quad (1)$$

$$\text{Vanillin yield (\%)} = \frac{\text{Moles of formed vanillin}}{\text{Initial moles of VA}} \times 100\% \quad (2)$$

$$\text{Vanillin selectivity (\%)} = \frac{\text{Vanillin yield}}{\text{Conversion}} \times 100\% \quad (3)$$

### 3. Results and discussion

#### 3.1. Catalyst characterization

Fig. 1 shows the XRD pattern of the calcined  $\text{Co}_3\text{O}_4$  catalyst recorded with a cobalt anode. All diffraction lines can be readily indexed according to the reference sample (JCPDS card 98-002-8158) for  $\text{Co}_3\text{O}_4$  having a cubic spinel structure (Fd-3m space group). The XRD pattern indeed confirmed the presence of the (111), (022), (113), (222), (004), (224) and (115)  $hkl$  reflections at  $2\theta = 22.11^\circ$ ,  $36.50^\circ$ ,  $43.09^\circ$ ,  $45.10^\circ$ ,  $52.59^\circ$ ,  $65.70^\circ$  and  $70.23^\circ$ , respectively. No additional XRD lines corresponding to other phases and/or unreacted cobalt nitrate were observed. The average crystallite size of the calcined  $\text{Co}_3\text{O}_4$  was estimated from the full width at half maximum of the (111), (113) and (115) XRD line by applying the Scherrer equation. A mean value of 6.3 nm was obtained which was far lower than that observed for the commercial  $\text{Co}_3\text{O}_4$  sample (86 nm). Such small size is to be related to the broadening of the XRD lines, which emphasizes the nanocrystalline nature of the spinel  $\text{Co}_3\text{O}_4$  catalyst.

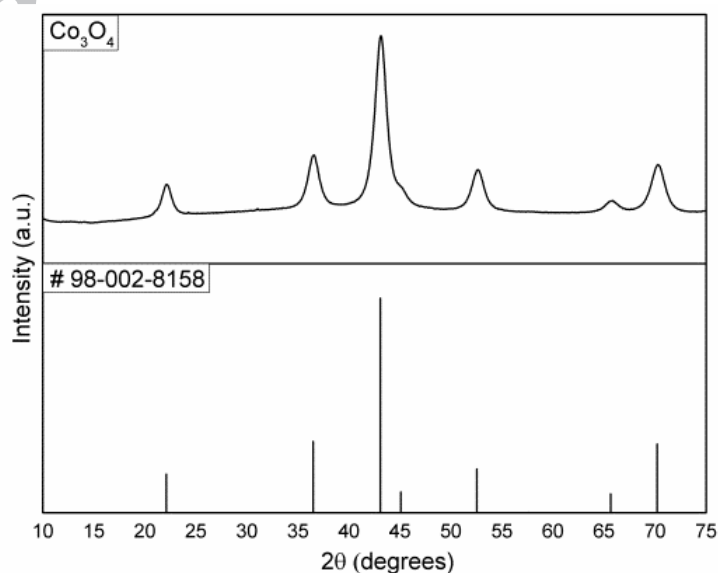


**Fig. 1.** XRD patterns of the calcined nanostructured  $\text{Co}_3\text{O}_4$  sample and the reference  $\text{Co}_3\text{O}_4$ .



The N<sub>2</sub> adsorption-desorption isotherm of the Co<sub>3</sub>O<sub>4</sub> sample and its corresponding pore size distribution are shown in Fig. 2. According to the IUPAC classification, the isotherm is of Type IVa and is attributed to a mesoporous material [26]. The capillary condensation is accompanied by hysteresis that starts to occur for pores wider than ~ 4 nm [26]. The shape of the isotherm exhibits a long adsorption plateau typical of the capillary condensation in the mesopores. The Type H1 hysteresis loop (IUPAC) is readily attributed to the presence of uniform mesopores with a narrow range, in accordance with the shape of the pore size distribution. The calcined Co<sub>3</sub>O<sub>4</sub> nanoparticles exhibited a specific surface area of 155 m<sup>2</sup> g<sup>-1</sup> coupled to a pore volume of 0.41 cm<sup>3</sup> g<sup>-1</sup> and a mean pore diameter of 10.1 nm.

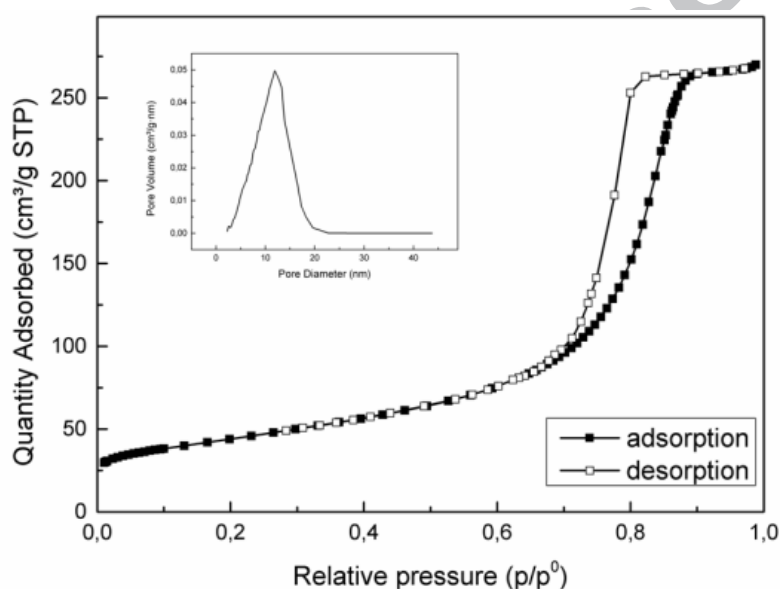


**Fig. 2.** N<sub>2</sub> adsorption-desorption isotherm for the calcined nanostructured Co<sub>3</sub>O<sub>4</sub> and the corresponding pore size distribution obtained from the adsorption branch (inset).

Representative SEM and HRTEM micrographs of the calcined Co<sub>3</sub>O<sub>4</sub> sample are displayed in Fig. 3. Scanning electron microscopy images (Fig. 3a and b) showed that the Co<sub>3</sub>O<sub>4</sub> sample was relatively porous and built up of aggregates consisting of primary particles that occurred non-isolated while forming a loose network. SEM EDS mapping of the calcined Co<sub>3</sub>O<sub>4</sub> catalyst revealed that the Co and O atoms were homogeneously distributed throughout the surface of the nanoparticles (Fig. S1 ESI). The light blue area in the carbon mapping corresponds to the carbon tape on which the sample was deposited prior to analysis. HRTEM analyses provided additional convincing evidence for the nanostructuration of the Co<sub>3</sub>O<sub>4</sub> sample. The size and morphology of the cobalt oxide particles were better depicted in Fig. 3c and d. TEM micrographs

revealed that the nanoparticles displayed a cubic morphology while being arranged in a roughly nanorod-like loosely structure. These particles exhibited a very small size varying between 5 and 10 nm, in agreement with the average crystallite size calculated by XRD (6.3 nm). Such results may also be correlated with the data obtained from nitrogen sorption analysis. The small size of the  $\text{Co}_3\text{O}_4$  nanoparticles coupled to their porous arrangement obviously account for their high developed surface area. The way they are arranged generates void (small cavities) whose mean diameter corresponds to the mean pore size determined by  $\text{N}_2$  adsorption-desorption measurements.

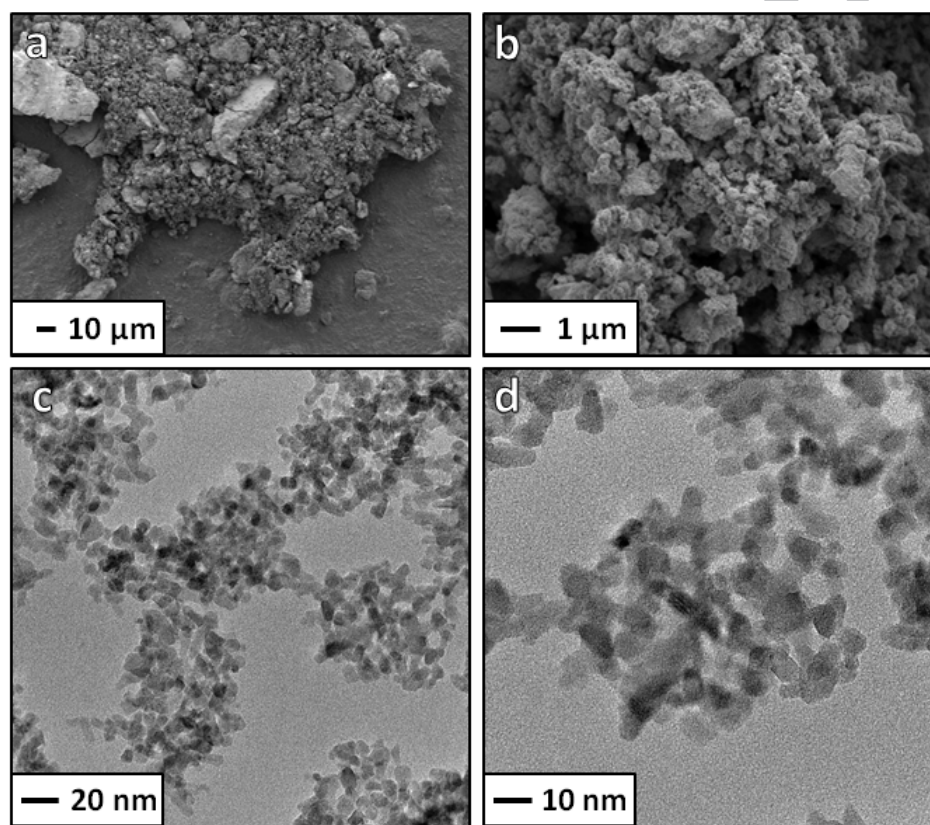


**Fig. 3.** Representative SEM (a-b) and HRTEM (c-d) micrographs of the calcined nanostructured  $\text{Co}_3\text{O}_4$  sample.

The formation of the spinel  $\text{Co}_3\text{O}_4$  was also duly confirmed by X-ray photoelectron spectroscopy (XPS). Such analysis was used to monitor the oxidation state and the relative percentage of the cobalt species in the  $\text{Co}_3\text{O}_4$  catalyst. As can be seen from Fig. S2 (ESI), two XPS signals were observed due to the  $\text{Co } 2p_{1/2}$  and  $\text{Co } 2p_{3/2}$  core level peaks at binding energies of 794.6 and 779.6 eV, respectively. A difference of 15 eV was observed corresponding to  $\text{Co}^{2+}$  and  $\text{Co}^{3+}$  species [27]. Both  $\text{Co } 2p_{1/2}$  and  $\text{Co } 2p_{3/2}$  peaks could be deconvoluted into three peaks.

Binding energies of 779.7, 781.0 and 782.3 eV were determined for the Co 2p<sub>3/2</sub> peak, ascribed to Co<sup>3+</sup> and Co<sup>2+</sup> species. Moreover, the surface composition calculated from XPS indicated that the atomic percentages of Co<sup>3+</sup> and Co<sup>2+</sup> were 67 and 33%, hence confirming the proper formation of the spinel oxide. Additionally, low intensity satellite peaks characteristic of Co<sub>3</sub>O<sub>4</sub> were also present [28].

The reducibility of the nanostructured spinel Co<sub>3</sub>O<sub>4</sub> was evaluated by temperature-programmed reduction. The H<sub>2</sub>-TPR profile was characterized by a two-step reduction process resulted from a progressive reduction of the Co<sub>3</sub>O<sub>4</sub> nanoparticles (Fig. S3 ESI). The first reduction peak was very sharp, symmetrical and centered at a temperature of 289 °C. This low-temperature peak corresponds to the reduction of Co<sub>3</sub>O<sub>4</sub> to divalent cobalt oxide (CoO), in accordance with literature data [29,30]. While being also almost symmetrical, the second reduction peak was broader with a temperature maximum located at 449 °C. This peak was associated to the subsequent reduction of CoO to metallic cobalt Co<sup>0</sup>. The observed maximum reduction temperature for both peaks was however far lower than that mentioned in the literature for similar cobalt oxides. The reduction of Co<sub>3</sub>O<sub>4</sub> to CoO (and hence CoO to Co<sup>0</sup>) was reported to be strongly dependent on the morphology and/or on the crystallites size of the initial Co<sub>3</sub>O<sub>4</sub> particles [29,31]. In the case of Co<sub>3</sub>O<sub>4</sub> nanoparticles, the reduction process into metallic cobalt started at 400°C and ended at 550°C, while for Co<sub>3</sub>O<sub>4</sub> nanotubes it only started at 500°C and was complete at 650°C. In our case, the lower maximum temperatures of the reduction peaks were obviously related to the small crystallite size of the calcined nanostructured Co<sub>3</sub>O<sub>4</sub> particles. All together, these observations (symmetrical shape, starting and ending reduction temperature values) are best corroborated with the morphological characteristics of the prepared Co<sub>3</sub>O<sub>4</sub> catalyst.

### *3.2. Selective oxidation of vanillyl alcohol over Co<sub>3</sub>O<sub>4</sub>*

#### *3.2.1. Optimization of experimental conditions*

The activity of the nanostructured spinel Co<sub>3</sub>O<sub>4</sub> catalyst was evaluated in the selective oxidation of vanillyl alcohol in terms of VA conversion (%) and yield to vanillin (%) by varying the experimental conditions under ultrasound activation during 15 min. Preliminary results indicated that the highest yields were generally obtained at this reaction time, according to the

obtained kinetic profiles that will be discussed later on (Fig. 7). The influence of the catalyst loading and hydrogen peroxide concentration on the catalytic properties was first investigated. In the absence of  $\text{Co}_3\text{O}_4$  catalyst, no vanillin was formed even if vanillyl alcohol conversion was observed, probably due to some substrate degradation (Fig. 4). The optimum catalyst loading was determined to be 2wt% of  $\text{Co}_3\text{O}_4$  related to the substrate. When higher amounts of catalyst were used in the reaction, the conversion increased until a plateau of 55%, whereas vanillin yields decreased. This is due to the overoxidation of vanillin that once formed, competes with the substrate for the oxidizing species available in the media. Such overoxidation issues will be discussed in the following sections.

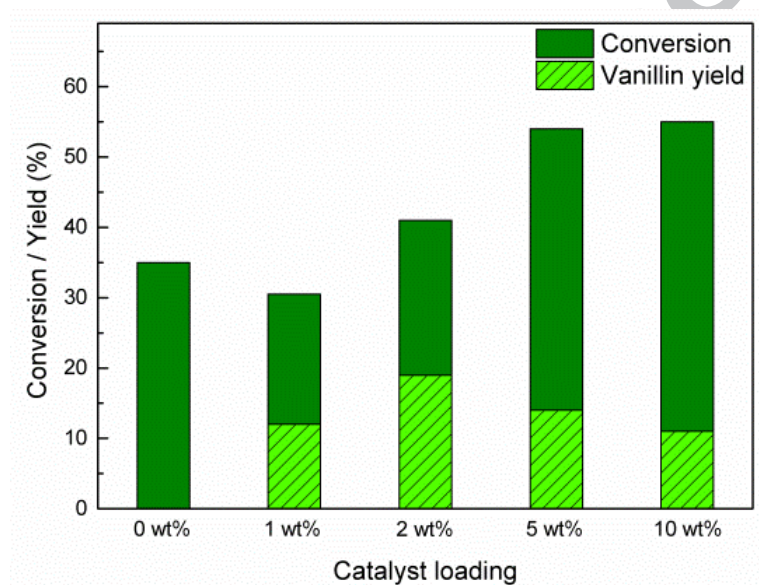


**Fig. 4.** Influence of the catalyst loading on the vanillyl alcohol oxidation (Experimental conditions:  $\text{Co}_3\text{O}_4$  as catalyst, 2 eq.  $\text{H}_2\text{O}_2$ , total volume of 4 mL (water), 20 kHz ultrasound, 75 °C, 15 min).

Interestingly, we observed that traces of vanillin are formed in the presence of the catalyst without  $\text{H}_2\text{O}_2$  addition (Fig. 5). This can be explained by the fact that ultrasound irradiation in water itself can generate *in situ* hydrogen peroxide and hence hydroxyl radicals [32], leading to some vanillin formation in the presence of the catalyst. Note that this effect was not observed in the absence of catalyst. In addition, increasing the amount of  $\text{H}_2\text{O}_2$  added into the reaction over 2 equivalents resulted in higher VA conversions but lower selectivities to vanillin due to the substrate and/or vanillin degradation/overoxidation. It was also noticed that the portionwise addition of  $\text{H}_2\text{O}_2$  in order to better control its consumption and reactivity in the reaction medium

did not improve the catalytic results under our conditions in the presence of the  $\text{Co}_3\text{O}_4$  catalyst (Fig. S4 ESI). This observation will be explained later on, in view of the understanding of the reactivity of this catalytic system under the investigated aqueous conditions.

By increasing the amount of catalyst or oxidant, the conversion of vanillyl alcohol increased, while the selectivity decreased. Gusevskaya *et al.* studied the selective oxidation of isoeugenol into vanillin using a vanadium homogeneous catalyst ( $n\text{-Bu}_4\text{NVO}_3$ ) [33]. The authors explained that as soon as a primary oxidation product undergoes further oxidation or degradation, the maximum yield is limited and depends on the rate in which the substrate and primary product get oxidized. Based on the rate constants  $k_1$  (first oxidation) and  $k_2$  (overoxidation) as well as on the reaction order, they calculated the maximum yield attained for the primary oxidation product. Thus, when  $k_1 = k_2$  in a first order reaction, the maximum yield to the primary product is theoretically 37% and only 25% when the primary product gets oxidized twice as fast as the substrate. The yield reaches 95% when the substrate reacts 100 times faster than the primary product [33]. In our case, neither vanillic acid nor hydroquinone was detected in the reaction medium. However, we observed the formation of few amounts of formic acid. The degradation pathway and the nature of the secondary oxidation products will be discussed in the last section.

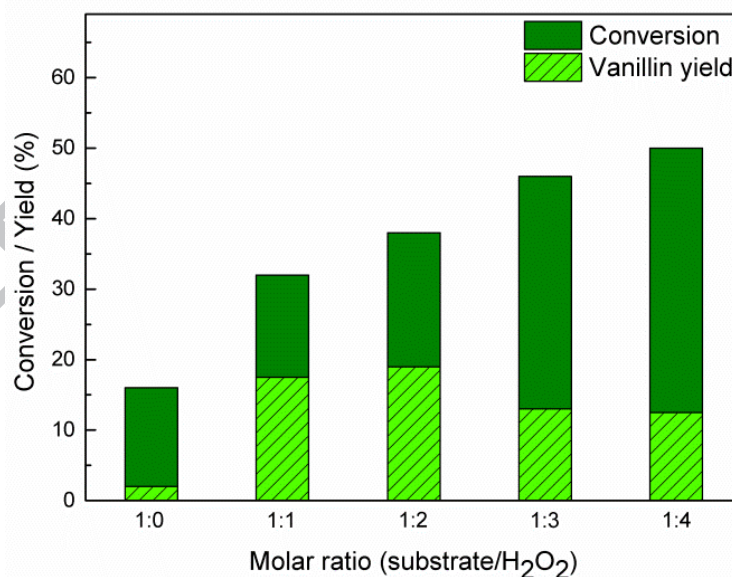


**Fig. 5.** Influence of the amount of oxidant on the vanillyl alcohol oxidation. (Experimental conditions: 2wt%  $\text{Co}_3\text{O}_4$ , 30%  $\text{H}_2\text{O}_2$  as oxidant, total volume of 4 mL (water), 20 kHz ultrasound, 75 °C, 15 min).



Along with the determination of the consumption of vanillyl alcohol as a function of time, we also determine that of vanillin as substrate. Fig. 6 clearly shows that both reaction rates were similar under these sonochemical conditions, thereby limiting the maximum yield to vanillin that can be reached.

In other words, high yields to vanillin are hard to be achieved if vanillin and vanillyl alcohol have similar oxidation rate constants. Under our optimal conditions with 2wt% catalyst and 2 molar equivalents of  $\text{H}_2\text{O}_2$  (30% aqueous solution), a maximum selectivity to vanillin of 50% corresponding to a yield of 19% could be attained (Table 1, Entry 4).

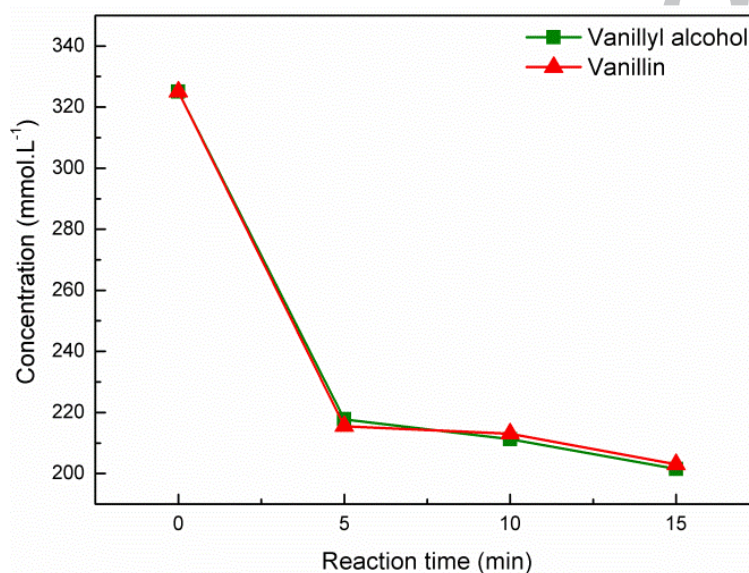


**Fig. 6.** Oxidation of vanillyl alcohol and vanillin as substrates under ultrasound (Experimental conditions: 2 wt%  $\text{Co}_3\text{O}_4$ , 2 eq. 30%  $\text{H}_2\text{O}_2$ , total volume of 4 mL (water), 20 kHz ultrasound, 75°C).

The stability of the nanostructured  $\text{Co}_3\text{O}_4$  catalyst was also evaluated in order to verify the absence of competitive homogeneous pathway during the oxidation reaction. For that purpose, the catalyst was separated from the aqueous medium at the end of the reaction and the filtrate solution was analyzed by ICP-OES to determine whether cobalt leaching occurred or not. The amount of cobalt in solution was shown to be negligible (<1.0wt%) for both activation systems. Moreover, the filtrate solution was not able to catalyze the reaction in a second run, thereby confirming that the oxidation process takes place through a heterogeneous pathway.

### 3.2.2. Ultrasonic vs. conventional conditions

The difference of reactivity between the sonochemical oxidation of vanillyl alcohol and the corresponding reaction under conventional heating (75 °C) is emphasized in Table 1. First, we checked that almost no conversion was observed in the absence of both the catalyst and the oxidant under ultrasound and silent conditions (Table 1, Entry 1). When H<sub>2</sub>O<sub>2</sub> was added in the absence of the Co<sub>3</sub>O<sub>4</sub> catalyst, no vanillin was obtained (Table 1, Entry 2). On the contrary, when the catalyst was added in the absence of any oxidant, no formation of vanillin occurred under conventional heating, while only traces were detected under ultrasound due to the interaction of the catalyst with few amounts of *in-situ* generated oxidative species (HO<sup>•</sup> and H<sub>2</sub>O<sub>2</sub>) (Table 1, Entry 3). The synergistic combination between Co<sub>3</sub>O<sub>4</sub>, hydrogen peroxide and ultrasonic activation was clearly highlighted by comparison with the reaction carried out under silent conditions (yield almost three times higher, Table 1, Entry 4). A commercial Co<sub>3</sub>O<sub>4</sub> nanopowder (Sigma-Aldrich) exhibiting a surface area of 32 m<sup>2</sup> g<sup>-1</sup> was also used for comparison purposes. While being far less efficient than the nanostructured spinel cobalt oxide we synthesized, again higher yield and selectivity to vanillin were obtained under ultrasonic irradiation than under silent conditions (Table 1, Entry 5), thereby confirming the synergistic “catalyst/oxidant/US” effect.

**Table 1**

Screening of different experimental conditions for vanillyl alcohol oxidation.

Entry	Experimental conditions <sup>a</sup>	Ultrasound (15 min)			Silent conditions (60 min)		
		Conv. (%)	Yield (%)	Select. (%)	Conv. (%)	Yield (%)	Select. (%)
1	Blank (without H <sub>2</sub> O <sub>2</sub> and Co <sub>3</sub> O <sub>4</sub> )	12	0	0	3	0	0
2	H <sub>2</sub> O <sub>2</sub> (2 eq.), without Co <sub>3</sub> O <sub>4</sub>	35	0	0	12	0	0
3	Co <sub>3</sub> O <sub>4</sub> (2 wt%), without H <sub>2</sub> O <sub>2</sub>	16	2	12	2	0	0
4	H <sub>2</sub> O <sub>2</sub> (2 eq.), Co <sub>3</sub> O <sub>4</sub> (2 wt%)	38	19	50	32	7	23
5	Same as entry 4 but with a commercial Co <sub>3</sub> O <sub>4</sub> (32 m <sup>2</sup> g <sup>-1</sup> )	28	5	18	24	1	5
Green chemistry metrics for entry 4		EF <sup>b</sup>		PMI <sup>b</sup>	EF <sup>b</sup>		PMI <sup>b</sup>
		12		111	35		302

<sup>a</sup> Experimental conditions: 1.3 mmol of vanillyl alcohol, total volume of 4 mL (water), 75 °C.

<sup>b</sup> E Factor (EF) and Process Mass Intensity (PMI) indexes defined in the ESI.

The kinetic profiles showed a maximum yield reached after 15 min under ultrasound (19%) and after 60 min under conventional heating (7%). It has to be noted that the total consumption of  $\text{H}_2\text{O}_2$  was observed after 5 min under ultrasound and after 15 min under conventional heating (Fig. S5 ESI). The VA oxidation kinetic profile under ultrasound is faster, but the degradation of vanillin is following the same trend under these conditions compared to the ones under conventional heating (Fig. 5 and Fig. S6 ESI).

Taking together, the catalytic results provided evidence that the reaction performed under low frequency ultrasound is faster than that under conventional heating conditions (15 min vs. 60 min to reach the maximum yield in vanillin), more selective (50% vs. 22%) and more efficient (19% vs. 7%). Moreover green metrics indicators such as the E Factor (EF) and the Process Mass Intensity (PMI) clearly show the benefit of the ultrasonic-mediated oxidation reaction (Table 1). Both the EF and PMI achieve a considerable decrease around 66% and 63% respectively. These results highlight the efficiency of the innovative combination between the heterogeneous catalyst ( $\text{Co}_3\text{O}_4$ ), the sonochemical activation method (20 kHz) and the eco-friendly oxidant ( $\text{H}_2\text{O}_2$ ) that are simultaneously used under mild conditions (low temperature and ambient pressure). Additionally, the real challenge here was to work in aqueous solution with the aim of developing a more sustainable oxidation process conforming to the principles of Green Chemistry. In this regard, we previously mentioned that only a few literature articles have described the catalytic selective oxidation of vanillyl alcohol using water as solvent, in particular when  $\text{H}_2\text{O}_2$  was used as O-donor, underlining the fact that further developments are still needed in this major field.

In summary, our results show that the ultrasound irradiation can improve reaction yields while decreasing reaction times, especially in water solution in the presence of  $\text{H}_2\text{O}_2$  and a heterogeneous catalyst compared to a conventional heating activation. Most importantly, the evaluation of the energy consumption confirmed that the proposed ultrasound-based catalytic system was eight times less energy consuming than that carried out under silent conditions (36 kJ vs. 288 kJ). Hence, such sonochemical-assisted heterogeneously catalyzed reaction proved to be a cost-effective oxidation process that should receive increasing level of interest in the future.



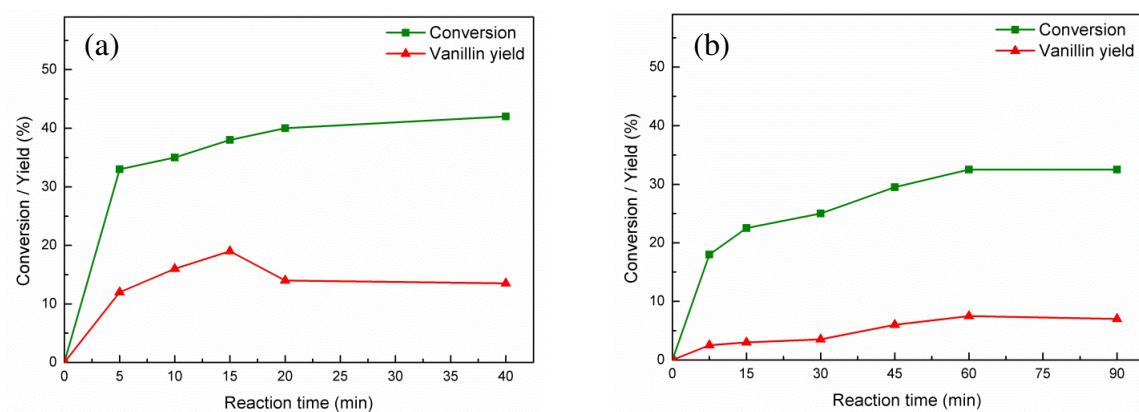


**Fig. 7.** Kinetic profiles of the selective oxidation of vanillyl alcohol a) under ultrasound and b) under unconventional heating (Experimental conditions: 2 wt%  $\text{Co}_3\text{O}_4$ , 2 eq. 30%  $\text{H}_2\text{O}_2$ , total volume of 4 mL (water), 75 °C).

In addition to the evaluation of the catalytic performances, we also investigated the mechanistic aspects of the reaction in order to explain the synergistic effects observed under low frequency ultrasound. First, it is clear that the reaction kinetics is increased by the physical effect of ultrasound, in particular through mass transfer and micro-mixing, improving the contact between the solid catalyst, the substrate and the oxidant within the solvent (heterogeneous system). From Fig. 7 and Fig. S5 (ESI), we can observe that the reaction pursued after the complete consumption of  $\text{H}_2\text{O}_2$  in both ultrasonic and conventional heating conditions. While it is well known that hydrogen peroxide can undergo Fenton-like reaction in the presence of cobalt species [34], generating  $\text{HO}^\bullet$  radicals that can assist the oxidation of VA into vanillin, our study also suggested that another oxidizing species is involved in the reaction mechanism. To assess the existence of chemical effects through the combined use of low frequency ultrasound and the catalyst in the presence of  $\text{H}_2\text{O}_2$ , the amount of hydroxyl radicals generated in the reaction medium was quantified by a potassium iodide dosimetry method. Compared to only irradiated water, the production of  $\text{HO}^\bullet$  was increased by a factor 10 in the presence of  $\text{H}_2\text{O}_2$ , and by a factor 10 as well in the presence of the catalyst in water (Table 2), confirming the increased production of hydroxyl under ultrasound/ $\text{Co}_3\text{O}_4$  conditions through a sono-Fenton-like reaction.

**Table 2**

Average formation of  $I_3^-$  under ultrasound ( $\text{mol s}^{-1}$ ) determined by KI dosimetry under ultrasound.

Entry	Time (min)	Experimental conditions <sup>a</sup>	Formation rate of $I_3^-$
1	5	$H_2O$	$2.4 \times 10^{-6}$
2	15	$H_2O$	$1.1 \times 10^{-6}$
3	5	$H_2O$ , $H_2O_2$ (2.6 mmol)	$1.1 \times 10^{-5}$
4	15	$H_2O$ , $H_2O_2$ (2.6 mmol)	$0.8 \times 10^{-5}$
5	5	$H_2O$ , $Co_3O_4$ (4 mg)	$3.7 \times 10^{-5}$
6	15	$H_2O$ , $Co_3O_4$ (4 mg)	$1.3 \times 10^{-5}$

<sup>a</sup> 0.1 mol.L<sup>-1</sup> aqueous KI solution (4 mL), 75 °C, ultrasound (20 kHz,  $P_{\text{acous.vol}} = 0.25 \text{ W mL}^{-1}$ )

However, the results gathered in Table 1 (Entry 2) showed that the  $HO^\bullet$  radicals formed *in-situ* were not responsible alone for the selective oxidation of vanillyl alcohol into vanillin. In addition, when the reaction was performed in acetonitrile a very low selectivity to vanillin (11%) was obtained, reaching a rapid plateau in terms of conversion (Fig. S7 ESI). Because in this case, no additional radical species were formed to pursue the reaction, no vanillin overoxidation was observed in acetonitrile after complete consumption of hydrogen peroxide, due to the same reasons.

Ali *et al.* investigated the selective oxidation of a lignin model compound through  $H_2O_2$  and a cobalt titanate in the presence of various solvents [15]. In terms of mechanisms, they proposed the formation of a hydroperoxyl group in interaction with the titanium within the cobalt titanate catalyst. Among the literature mechanisms describing the decomposition of  $H_2O_2$  through oxygen vacancies on the surface of transition metal oxides, the authors mentioned that a bond was formed between the catalyst oxygen surface vacancies and the oxygen stemming from  $H_2O_2$  ( $V_{\text{surf}}-O$ ) [35,36]. Other authors reported the formation of a superoxide  $O_2^{\bullet-}$  radical species [37] or suggested the formation of hydroperoxide, hydroxide or oxy species chemisorbed on the surface of cobalt based catalysts [23,38,39]. In our case, we evidenced by XPS analyses of (i) the catalyst itself, (ii) the catalyst reacting with  $H_2O_2$  under conventional heating, and (iii) the catalyst reacting with  $H_2O_2$  under sonochemical activation, that the O1s component at around 530.8–531 eV contribution increased in both cases (Fig. 8). Those values of binding energies may be assigned to a variety of oxygen species such as adsorbed  $O^-$  or OH-like species, while peaks at

higher binding energies, ranging from 531.4 to 532 eV, could be assigned to subsurface  $O^-$  species [40]. Peaks located at lower binding energies, in our case ranging from 329.6 to 530 eV, correspond to lattice oxygen. The ratio between oxygen surface species and lattice oxygen ( $O_{\text{surface}}/O_{\text{lattice}}$ ) was shown to increase from 0.28 for the parent  $\text{Co}_3\text{O}_4$  catalyst to 0.36 for  $\text{Co}_3\text{O}_4$  after reaction with  $\text{H}_2\text{O}_2$  under conventional heating and to 0.53 for  $\text{Co}_3\text{O}_4$  that reacted with  $\text{H}_2\text{O}_2$  under ultrasonic conditions.

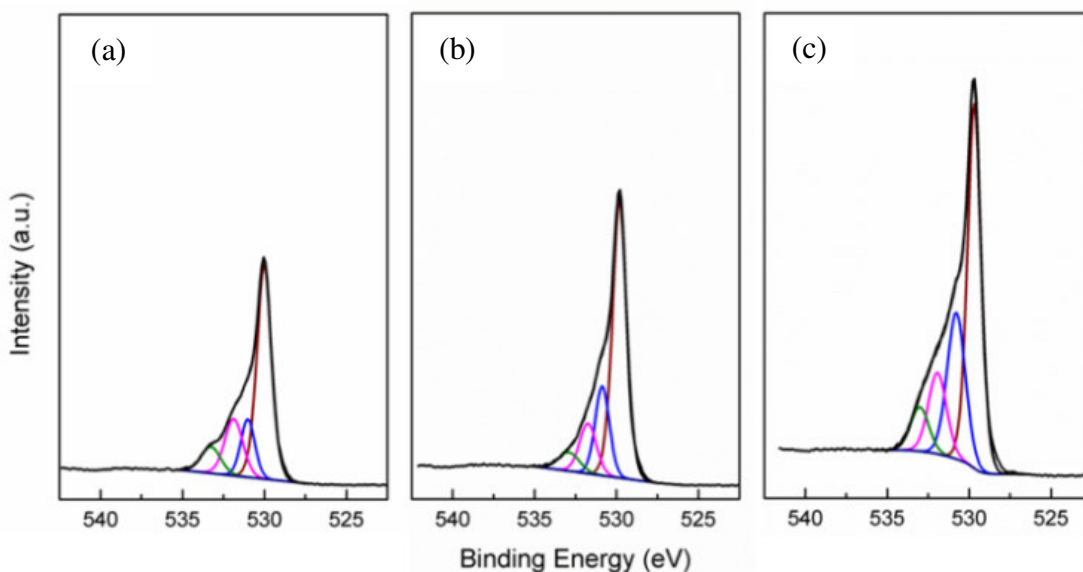


**Fig. 8.** O1s X-ray photoelectron spectroscopy (XPS) of (a)  $\text{Co}_3\text{O}_4$ , (b)  $\text{Co}_3\text{O}_4$  after treatment with  $\text{H}_2\text{O}_2$  under conventional heating and (c)  $\text{Co}_3\text{O}_4$  after treatment with  $\text{H}_2\text{O}_2$  under ultrasound.

This result suggests that such surface species might be the oxidizing species involved in the selective VA oxidation reaction mechanism. Further investigations are currently being conducted in our lab to better understand this mechanism.

### 3.2.3. Catalyst poisoning

At the end of both US- and CH-assisted vanillyl alcohol oxidations, a higher mass of catalyst was collected than the one engaged for the reactions, suggesting the presence of a carbonaceous deposit. TGA analyses of the recovered catalyst (by filtration) indicated a mass loss of about 30 wt%, along with the initial mass loss corresponding to physisorbed water, independently of the activation method used for the VA oxidation reaction (Fig. S8 ESI). Scanning electron microscopy mapping images of both  $\text{Co}_3\text{O}_4$  samples after reaction were then

carried out with the aim of characterizing the catalyst environment. The comparison of Co, O, and C EDS mapping of the used catalyst after the ultrasonic reaction revealed the presence of carbon species admixed with the catalyst particles (Fig. 9), thereby confirming that they were contaminated with a carbonaceous deposit during the oxidation reaction. The same behavior was observed for the  $\text{Co}_3\text{O}_4$  catalyst after the reaction performed under conventional heating (Fig. S9 ESI).

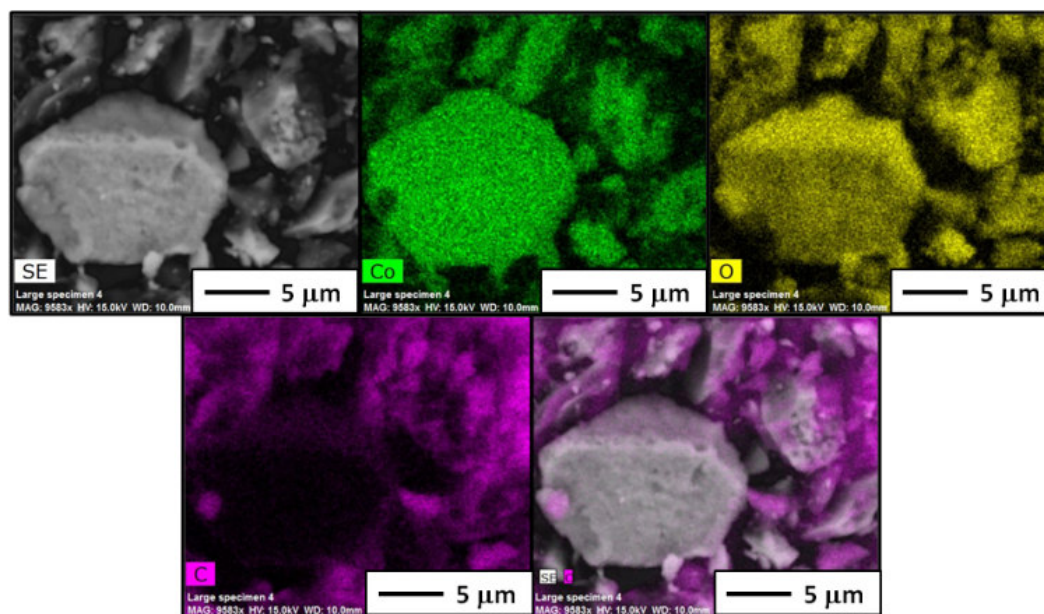


**Fig. 9.** EDS mapping of the recovered  $\text{Co}_3\text{O}_4$  catalyst at the end of the ultrasound-assisted reaction (Experimental conditions: 2 wt%  $\text{Co}_3\text{O}_4$ , 2 eq. 30%  $\text{H}_2\text{O}_2$ , 20 kHz, total volume of 4 mL (water), 75 °C).

CHNS elemental analysis of the post-reaction catalyst under CH activation indicated a total carbon + hydrogen content of about 25 wt%, in the same order as the mass loss determined by TGA. In an attempt to remove the admixed carbonaceous species, the used catalyst was further calcined at 300 °C under air for 2 h. However, a significant residual carbon + hydrogen content (~ 11 wt%) was still observed, suggesting that a higher calcination temperature is required to eliminate this deposit.

GC-MS and MALDI-TOF analyses were further carried out, in order to identify the nature of the carbonaceous deposit admixed with the  $\text{Co}_3\text{O}_4$  catalyst. The catalyst was washed with dichloromethane and first analyzed by GC-MS. Such analyses indicated the presence of traces of vanillyl alcohol and vanillin (about 25 ppm). The analysis by MALDI-TOF of the

dichloromethane washed catalyst solution (Fig. S10 ESI) pointed out the presence of relatively high molecular weight compounds adsorbed at the surface of the catalyst. According to these analyses and to literature data, it is suggested that uncontrolled oligomerization of aromatics compounds occurred in such oxidative reaction medium [41]. For instance, the Dakin oxidation is a well-known reaction, in which an aromatic aldehyde such as vanillin, gets oxidized by  $\text{H}_2\text{O}_2$  to the corresponding hydroquinone [42], which can easily undergo further reactions through polymerization. The oxidation products can rapidly form larger colored oligomers through further oxidation reactions in water [41]. Despite the fact that we did not observe hydroquinone in our reaction medium analyses, we did confirm the presence of high molecular weight compounds through MALDI-TOF. Such adsorbed oligomers onto the surface of the catalyst contribute to its poisoning, thereby hampering its recyclability. All these data demonstrate the complexity of the heterogeneous oxidation reaction carried out with  $\text{H}_2\text{O}$  as solvent and hydrogen peroxide as the primary oxidant. The operational parameters (such as the nature of the solid catalyst, the mode of addition of  $\text{H}_2\text{O}_2$ , sustainable biphasic systems) deserve careful attention, so as to increase the yield to the desired product and to avoid undesirable oligomerization side reactions. Further researches are currently being undertaken to this end in our lab in order to limit these recycling issues, while increasing the catalytic efficiency.

#### 4. Conclusions

In this paper, the challenge was to perform the catalytic oxidation of vanillyl alcohol to vanillin under milder reaction conditions than those generally used in the literature. Working under mild conditions (hydrogen peroxide, low temperature, ambient pressure) while promoting the mass transfer in a heterogeneously catalyzed system, requires the employment of specific activation methods, such as ultrasound irradiation. Ultrasound generated in aqueous medium indeed favors the production of hydroxyl radicals through *in situ* formation of  $\text{H}_2\text{O}_2$  (chemical effects), as well as the increase of mass transfer between the  $\text{Co}_3\text{O}_4$  catalyst and the organic substrate (physical effects). Such sono-Fenton-like mediated selective oxidation proved to be more efficient than the reaction carried out under conventional heating owing to synergistic effects between the ultrasound,  $\text{H}_2\text{O}_2$  and the solid catalyst. A vanillyl alcohol conversion of 38% was reached after only 15 min of reaction under US conditions with a selectivity to vanillin of 50%. Even if further improvements are still needed, the novelty of this work relies on the



coupling of a non-noble metal based heterogeneous catalyst with a sonochemical activation method for the oxidation of a lignin model compound under more eco-friendly conditions, especially when the challenging use of water as solvent is concerned. The ultrasound-assisted H<sub>2</sub>O<sub>2</sub> catalytic oxidation of vanillyl alcohol into vanillin in water proved to be faster (4x), more selective (2.3x) and more efficient (2.7x) than the corresponding reaction under silent conditions. Additionally, a far decrease of the energy consumption of the reaction was observed under ultrasound (36 kJ vs. 288 kJ). This preliminary work opens the door for further investigations in heterogeneously catalyzed sono-Fenton-like-assisted reactions in order to develop greener selective oxidation processes in the future.

### Acknowledgements

The authors gratefully acknowledge the CAPES Foundation (Brazilian Ministry of Education) for the awarding of the PhD scholarship (13342-13-4) to Ronan Behling through the *Science without Borders* program. The authors are also very much indebted to the technical assistance from the research support services of LNEC and IC2MP (University of Poitiers, France), in particular to E. Beré, S. Pronier, S. Arrii-Clacens, C. Canaff and M. Tarighi for recording the SEM, TEM, XRD, XPS and MALDI-TOF analyses, respectively.

### References

- 
- [1] R. Behling, S. Valange, G. Chatel, Heterogeneous catalytic oxidation for lignin valorization into valuable chemicals: what results? What limitations? What trends?, *Green Chem.* 18 (2016) 1839–1854.
  - [2] M. Fache, B. Boutevin, S. Caillol, Vanillin Production from Lignin and Its Use as a Renewable Chemical, *ACS Sustainable Chem. Eng.* 4 (2016) 35–46.
  - [3] E. de Jong, W. J. van Berkel, R. P. van der Zwan, J. A. de Bont, Purification and characterization of vanillyl-alcohol oxidase from *Penicillium simplicissimum*. A novel aromatic alcohol oxidase containing covalently bound FAD, *Eur. J. Biochem.* 208 (1992) 651–657.
  - [4] M. Lahtinen, P. Heinonen, M. Oivanen, P. Karhunen, K. Kruus, J. Sipilä, On the factors affecting product distribution in laccase-catalyzed oxidation of a lignin model compound vanillyl alcohol: experimental and computational evaluation, *Org. Biomol. Chem.* 11 (2013) 5454–5464.

- [5] A. Sharma, S. C. Verma, N. Saxena, N. Chadda, N. P. Singh, A. K. Sinha, Microwave- and ultrasound-assisted extraction of vanillin and its quantification by high-performance liquid chromatography in *Vanilla planifolia*, *J. Sep. Sci.* 29 (2006) 613–619.
- [6] C. Valdez-Flores, M.P. Cañizares-Macias, On-line dilution and detection of vanillin in vanilla extracts obtained by ultrasound, *Food Chem.* 105 (2007) 1201–1208.
- [7] D. Jadhav, B. N. Rekha, P. R. Gogate, V. K. Rathod, Extraction of vanillin from vanilla pods: A comparison study of conventional soxhlet and ultrasound assisted extraction, *J. Food Eng.* 93 (2009) 421–426.
- [8] J. Zakzeski, P. C. Bruijninx, A. L. Jongerius, B. M. Weckhuysen, The catalytic valorization of lignin for the production of renewable chemicals, *Chem. Rev.* 110 (2010) 3552–3599.
- [9] A. Jha, D. Mhamane, A. Suryawanshi, S. M. Joshi, P. Shaikh, N. Biradar, S. Ogale, C. V. Rode, Triple nanocomposites of  $\text{CoMn}_2\text{O}_4$ ,  $\text{Co}_3\text{O}_4$  and reduced graphene oxide for oxidation of aromatic alcohols, *Catal. Sci. Technol.*, 4 (2014) 1771–1778.
- [10] J. C. Colmenares, R. Luque, Heterogeneous photocatalytic nanomaterials: prospects and challenges in selective transformations of biomass-derived compounds, *Chem. Soc. Rev.* 43 (2014) 765–778.
- [11] S-H. Li, S. Liu, J. C. Colmenares, Y-J. Xu, A sustainable approach for lignin valorization by heterogeneous photocatalysis, *Green Chem.* 18 (2016) 594–607.
- [12] V. Augugliaro, G. Camera-Roda, V. Loddo, G. Palmisano, L. Palmisano, F. Parrino, M. A. Puma, Synthesis of vanillin in water by  $\text{TiO}_2$  photocatalysis, *Appl. Catal., B.* 111–112 (2012) 555–561.
- [13] C. Crestini, M. C. Caponi, D. S. Argyropoulos, R. Saladino, Immobilized methyltrioxo rhenium (MTO)/ $\text{H}_2\text{O}_2$  systems for the oxidation of lignin and lignin model compounds, *Biorg. Med. Chem.* 14 (2006) 5292–5302.
- [14] S. Stolte, H. T. T. Bui, S. Stedte, V. Korinth, J. Arning, A. Białk-Bielińska, U. Bottin-Weber, M. Cokoja, A. Hahlbrock, V. Fetz, R. Stauber, B. Jastorff, C. Hartmann, R. W. Fischer, F. E. Kühn, Preliminary toxicity and ecotoxicity assessment of methyltrioxorhenium and its derivatives *Green Chem.* 17 (2015) 1136–1144.
- [15] M. Shilpy, M. Ali Ehsan, T. Hussein Ali, S. Bee Abd Hamid, Md. Eaqub Ali, Performance of cobalt titanate towards  $\text{H}_2\text{O}_2$  based catalytic oxidation of lignin model compound, *RSC Adv.* 5 (2015) 79644–79653.
- [16] X. Gu, M. He, Y. Shi, Z. Li, La-containing SBA-15/ $\text{H}_2\text{O}_2$  systems for the microwave assisted oxidation of a lignin model phenolic compound, *Maderas Cienc. Tecnol.* 12 (2010) 181–188.
- [17] T. J. Mason, Sonochemistry and sonoprocessing: the link, the trends and (probably) the future, *Ultrason. Sonochem.* 10 (2003) 175–179.
- [18] G. Cravotto, P. Cintas, Forcing and Controlling Chemical Reactions with Ultrasound, *Angew. Chem., Int. Ed.*, 46 (2007) 5476–5478.
- [19] K. S. Suslick, D. A. Hammerton, D. E. Cline, Sonochemical hot spot, *J. Am. Chem. Soc.* 108 (1986) 5641–5645.
- [20] G. Chatel, Sonochemistry – New opportunities for green chemistry, Word Scientific: London, UK, 2016, 200 p.
- [21] P. Cintas, J.-L. Luche, Green chemistry. The sonochemical approach, *Green Chem.* 1 (1999) 115–125.

- [22] S. Chakma, V. S. Moholkar, Physical mechanism of sono-Fenton process, *AIChE J.* 59 (2013) 4303–4313.
- [23] V. R. Mate, A. Jha, U. D. Joshi, K. R. Patil, M. Shirai, C. V. Rode, Effect of preparation parameters on characterization and activity of  $\text{Co}_3\text{O}_4$  catalyst in liquid phase oxidation of lignin model substrates, *Appl. Catal. A: Gen.* 487 (2014) 130–138.
- [24] S. Koda, T. Kimura, T. Sakamoto, T. Kondon, H. Mitome, A standard method to calibrate sonochemical efficiency of an individual reaction system, *Ultrason. Sonochem.* 10 (2003) 149–156.
- [25] S. La Rochebrochard d'Auzay, J.-F. Blais, E. Naffrechoux, Comparison of characterization methods in high frequency sonochemical reactors of differing configurations, *Ultrason. Sonochem.* 17 (2010) 547–554.
- [26] M. Thommes, K. Kaneko, A. V. Neimark, J. P. Oliver, F. Rodriguez-Reinero, J. Rouquerol, K. S. W. Sing, Physisorption of gases, with special reference to the evaluation of surface area and pore size distribution (IUPAC Technical Report), *Pure Appl. Chem.* 87 (2015) 1051–1069.
- [27] L.F. Liotta, G. D. Carlo, G. Pantaleo, A. M. Venezia, G. Deganello,  $\text{Co}_3\text{O}_4/\text{CeO}_2$  composite oxides for methane emissions abatement: Relationship between  $\text{Co}_3\text{O}_4$ – $\text{CeO}_2$  interaction and catalytic activity, *Appl. Catal., B* 66 (2006) 217–227.
- [28] B. Tan, K. J. Klabunde, P. M. A. Sherwood, XPS studies of solvated metal atom dispersed (SMAD) catalysts. Evidence for layered cobalt-manganese particles on alumina and silica, *J. Amer. Chem. Soc.* 113 (1991) 855–861.
- [29] A. Jha, C. V. Rode, Highly selective liquid-phase aerobic oxidation of vanillyl alcohol to vanillin on cobalt oxide ( $\text{Co}_3\text{O}_4$ ) nanoparticles, *New J. Chem.* 37 (2013) 2669–2674.
- [30] P. Arnoldy, J. A. Moulijn, Temperature-programmed reduction of  $\text{CoOAl}_2\text{O}_3$  catalysts, *J. Catal.* 93 (1985) 38–54.
- [31] B. Guillot, M. Laarj, P. Tailhades, A. Rousset, Effect of crystallite size on oxidation and reduction behavior of a manganese substituted magnetite of composition  $\text{Mn}_{0.67}\text{Fe}_{2.33}\text{O}_4$ , *Mater. Chem. Phys.* 19 (1988) 485–495.
- [32] X. Fang, G. Mark, C. von Sonntag, OH radical formation by ultrasound in aqueous solutions Part I: the chemistry underlying the terephthalate dosimeter, *Ultrason. Sonochem.* 3 (1996) 57–63.
- [33] E. V. Gusevskaya, L. Menini, L. A. Parreira, R. A. Mesquita, Y. N. Kozlov, G. B. Shul'pin, Oxidation of isoeugenol to vanillin by the “ $\text{H}_2\text{O}_2$ –vanadate–pyrazine-2-carboxylic acid” reagent, *J. Mol. Catal. Chem.* 363–364 (2012) 140–147.



- [34] A. D. Bokare, W. Choi, Review of iron-free Fenton-like systems for activating H<sub>2</sub>O<sub>2</sub> in advanced oxidation processes, *J. Hazard. Mater.* 275 (2014) 121–135.
- [35] R. C. C. Costa, M. F. F. Lelis, L. C. A. Oliveira, J. D. Fabris, J. D. Ardisson, R. R. V. A. Rios, C. N. Silva, R. M. Lago, Novel active heterogeneous Fenton system based on Fe<sub>3-x</sub>M<sub>x</sub>O<sub>4</sub> (Fe, Co, Mn, Ni): the role of M<sup>2+</sup> species on the reactivity towards H<sub>2</sub>O<sub>2</sub> reactions, *J. Hazard. Mater.* B129 (2006) 171–178.
- [36] Y. N. Lee, R. M. Lago, J. L. G. Fierro, J. Gonzalez, Hydrogen peroxide decomposition over Ln<sub>1-x</sub>A<sub>x</sub>MnO<sub>3</sub> (Ln = La or Nd and A = K or Sr) perovskites, *Appl. Catal., A* 215 (2001) 245–256.
- [37] L. V. L. Lupano, J. M. L. Martinez, L. L. Piehl, E. R. de Celis, V. C. Dall’Orto, Activation of H<sub>2</sub>O<sub>2</sub> and superoxide production using a novel cobalt complex based on a polyampholyte, *Appl. Catal., A* 467 (2013) 342–354.
- [38] P. Visuvamithiran, B. Sundaravel, M. Palanichamy, V. Murugesan, Oxidation of alkyl aromatics over SBA-15 supported cobalt oxide, *J. Nanosci. Nanotechnol.* 13 (2013) 2528–2537.
- [39] A. M. I. Jayaseeli, A. Ramdass, S. Rajagopal, Selective H<sub>2</sub>O<sub>2</sub> oxidation of organic sulfides to sulfoxides catalyzed by cobalt(III)–salen ion, *Polyhedron* 100 (2015) 59–66.
- [40] A. Amri, X. F. Duan, C. Yin, Z. Jiang, M. M. Rahman, T. Pryor, Solar absorptance of copper–cobalt oxide thin film coatings with nano-size, grain-like morphology: Optimization and synchrotron radiation XPS studies, *Appl. Surf. Sci.* 275 (2013) 127–135.
- [41] K. Robards, P. D. Prenzler, G. Tucker, P. Swatsitang, W. Glover, Phenolic compounds and their role in oxidative processes in fruits, *Food Chem.* 66 (1999) 401–436.
- [42] M. Fache, E. Darroman, V. Besse, R. Auvergne, S. Caillol, B. Boutevin, Vanillin, a promising biobased building-block for monomer synthesis, *Green Chem.* 16 (2014) 1987–1998.

**HIGHLIGHTS****Sonochemical selective oxidation of vanillyl alcohol in the presence of a cobalt oxide catalyst under mild conditions**

Ronan Behling, Gregory Chatel\* and Sabine Valange\*

- 1) Catalytic selective oxidation of vanillyl alcohol into vanillin under mild conditions.
- 2) Coupling of a solid catalyst with low frequency ultrasonic irradiation in aqueous medium.
- 3) Nanostructured spinel  $\text{Co}_3\text{O}_4$  prepared and characterized before and after reaction.
- 4) Reaction performed at ambient pressure, low temperature, with  $\text{H}_2\text{O}_2$  as oxidant.
- 5) US- $\text{H}_2\text{O}_2$  process faster and more selective than that performed under silent conditions.